ACCSCIENCE PUBLISHING

Tumor Discovery

ORIGINAL RESEARCH ARTICLE

A novel gene prognostic signature lymphocyte cytosolic protein 2 regulates melanoma progression by activating tumor-infiltrating CD8+ T-cells through the interferon regulatory factor 5 signaling pathway

Hongyin Sun[1,2,3†], Kui Deng[4†], Xingchen Zhou[1,2†], Dongsheng Cao[5], Yan Cheng[6], Xiang Chen[1,2*], and Mingzhu Yin[1,2*]

[1]Department of Dermatology, Hunan Engineering Research Center of Skin Health and Disease, Hunan Key Laboratory of Skin Cancer and Psoriasis, Xiangya Hospital, Central South University, Changsha, China

[2]National Clinical Research Center for Geriatric Disorders, Xiangya Hospital, Central South University, Changsha, China

[3]Department of Pharmacy, Shantou University Medical College, Shantou University, Shantou, China

[4]Key Laboratory of Growth Regulation and Translational Research of Zhejiang Province, School of Life Sciences, Westlake University, 18 Shilongshan Rd, Cloud Town, Hangzhou, China

[5]Department of Pharmacy, Xiangya Hospital, Central South University, Changsha, Hunan, China

[6]Department of Pharmacy, The Second Xiangya Hospital, Central South University, Changsha, China

[†]These authors contributed equally to this work.

***Corresponding authors:**
Xiang Chen
(chenxiangck@126.com)
Mingzhu Yin
(yinmingzhu@csu.edu.cn)

Citation: Sun H, Deng K, Zhou X, *et al*., 2023, A novel gene prognostic signature lymphocyte cytosolic protein 2 regulates melanoma progression by activating tumor-infiltrating CD8+ T-cells through the interferon regulatory factor 5 signaling pathway. *Tumor Discov*, 2(1): 318.
https://doi.org/10.36922/td.318

Received: December 29, 2022
Accepted: February 27, 2023
Published Online: March 24, 2023

Copyright: © 2023 Author(s). This is an Open Access article distributed under the terms of the Creative Commons Attribution License, permitting distribution, and reproduction in any medium, provided the original work is properly cited.

Publisher's Note: AccScience Publishing remains neutral with regard to jurisdictional claims in published maps and institutional affiliations.

Abstract

Cutaneous malignant melanoma is the most lethal skin cancer. The advent of immunotherapy has revolutionized the status of clinical therapies of melanoma, which brought new hope to these patients. However, only a small proportion of patients are responders. Therefore, the identification of novel prognostic and immune-related biomarkers is crucial to guide the development of melanoma clinical treatments. Herein, RNA-seq data of the cutaneous melanoma from public database were used for identifying prognostic gene signatures, and we found that high expression of lymphocyte cytosolic protein 2 (LCP2) in melanoma patient was significantly associated with better prognosis for melanoma. Kyoto Encyclopedia of Genes and Genomes and gene ontology analyses demonstrated that the differentially expressed genes are significantly involved in lysosome, B-cell receptor signaling pathways, Fc epsilon RI signaling pathway, and T-cell receptor signaling pathway, indicating that these signaling pathways play important roles in melanoma. LCP2 expression was positively correlated with CD8+ T-cell and the overall survival of melanoma patients, and this positive correlation was directly confirmed by fluorescence-activated cell sorting experiment. The *in vivo* experiment showed that LCP2 knockdown significantly promoted the melanoma progression and decreased interferon regulatory factor 5 (IRF5) expression. In conclusion, we identified that LCP2 is a possible prognostic gene signature for progression-free survival of melanoma patients and regulates melanoma progression by activating tumor-infiltrating CD8+ T-cells through the IRF5 signaling pathway, indicating that LCP2 could serve as a prognostic biomarker and therapeutic target in immunotherapy.

Keywords: Cutaneous melanoma; Lymphocyte cytosolic protein 2; Prognostic gene signature; Immunotherapies; Interferon regulatory factor 5

1. Introduction

Melanoma is known to be the most lethal type of skin cancer, with an estimated over 160,000 new cases diagnosed each year[1,2]. Although melanoma constitutes <5% of all skin cancers, 80% of skin cancer-related deaths are caused by melanoma. Despite great advances in biological research and therapeutic approaches in the past years, the morbidity and mortality rates have still increased in the past half century[2]. Due to high immunogenicity of melanoma, the recent breakthroughs achieved in immunotherapies have revolutionized the way we treat melanoma, and this has led to a dramatic improvement in the prognosis of the patients[3,4]. However, only a small proportion of patients respond to these immunotherapies, which means that the mechanism of interaction between immune system and melanoma invasion has not yet been fully elucidated. Therefore, it is necessary to identify transcriptome signatures within tumor immune microenvironment that affects tumor progression and patient survival.

Several studies have successfully identified transcriptome signatures that could predict the survival of melanoma patients[5,6]. These signatures could help discern melanoma patients with high risk in advance and evaluate response to certain therapeutic interventions. Few studies have explored the relationship between the immune gene expression and the prognosis for melanoma. Zhao *et al.* identified a 25-gene signature from immune cells-related genes though selecting the genes with the highest correlation with the ImmuneScore that reflects leukocyte infiltration, and calculated leukocyte infiltration score to predict the survival of melanoma patients[7]. However, not all 25 genes identified in this study may be associated with the development and progression of melanoma.

Lymphocyte cytosolic protein 2 (LCP2), one of the SLP-76 family of adapters, is primarily expressed in hematopoietic cells[8]. In addition, LCP2 is also reported to be expressed in platelets, macrophages, neutrophils, mast cells, developing B-cells, and natural killer cells[8,9]. However, the current data showed that LCP2 is differentially expressed in many different types of tumors and is correlated with prognosis in gastric cancer, breast cancer[10], lung adenocarcinoma,[11] and metastatic melanoma[12] patients. Furthermore, it has been reported that LCP2 is involved in T-cell-receptor signaling[13] and is essential for normal T-cell development and activation[14]. LCP2 can activate the promoter of interleukin (IL)-2 through promoting the activation of T-cell, and IL-2 secretion subsequently results in the release of cytokines that lead to apoptosis of target cells[15,16]. Moreover, Siggs *et al.* found that the mice with LCP2 mutation secreted excessive amounts of proinflammatory cytokines, IgE, and autoantibodies, suggesting that slight decrease in LCP2 expression is enough to trigger immune dysregulation[17]. In a nutshell, LCP2 plays a significant important role in the immune system. However, the specific role of LCP2 in the tumor microenvironment is still obscure.

As melanoma exhibits high immunogenicity, we hypothesized that identifying immune-related genes that are associated with the occurrence and prognosis of melanoma could help delineate the melanoma-specific mechanisms of immunoregulation, which may shed new light on immunotherapy research. In the present study, the RNA-seq data of cutaneous melanoma from the public database were used for identifying prognostic gene signatures, and we found that LCP2 was highly expressed in the patients with melanoma. The expression of LCP2 was positively correlated with $CD8^+$ T-cell and the overall survival (OS) of melanoma patients, and this positive correlation was directly confirmed by flow cytometry analysis. Moreover, we further explored the potential mechanism of LCP2 in tumor microenvironment of melanoma *in vivo*. Knockdown of LCP2 significantly promoted the progression of melanoma and decreased the IRF5 expression. Based on our results, we identified that LCP2 is a possible prognostic gene signature for progressive-free survival of patients with melanoma, which repressed the growth of melanoma through positively regulating the IRF5 signaling pathway followed by activation of $CD8^+$ T-cells and promotion of antitumor response.

2. Materials and methods

Major immune pathways (N = 29) were retrieved from the Reactome pathway database (https://reactome.org/)[18], which contains three main immune pathways including innate immune system, adaptive immune system, and cytokine signaling in immune system, and 2070 genes in total.

2.1. Data sets used

We used two expression profile data sets to identify differentially expressed genes (DEGs) between melanomas and controls. These data sets are GSE3189 (including 45 melanoma samples, 18 benign skin nevus samples, and seven normal skin samples) and GSE31879 (including ten

melanoma samples and four normal melanocyte samples). GSE15605 (including 58 melanoma samples and 16 normal skin samples) was used to validate the identified DEGs. The RNA-seq data of cutaneous melanoma from the Cancer Genome Atlas (TCGA) were downloaded from the UCSC Cancer Brower (https://xenabrowser.net/), which contained 471 melanoma samples. The TCGA RNA-seq data were utilized to further identify prognostic genes that could predict the survival of melanoma, and to construct prognostic models. In addition, GSE65904, which contains 214 melanoma samples, was used to validate the identified prognostic gene signatures. Variables with missing values >20% of all samples were excluded from this study, and the remaining missing values were imputed by nearest neighbor averaging method using the R package *impute*[19]. The characteristics of the five data sets used in our study are provided in Table S1.

2.2. Identification and validation of DEGs

GSE3189 and GSE31879 data sets were used to select DEGs. DEGs between melanoma and benign skin nevus, melanoma and normal skin tissue, melanoma, and normal melanocyte were screened by Wilcoxon rank-sum test, separately. The false discovery rate (FDR) method was used to correct type I error occurring when conducting multiple comparison[20]. Variables with q value generated by FDR <0.01 were selected, and the DEGs that were shared between melanoma and three controls (nevus, normal skin, and melanocyte) were screened as the robust DEGs. The robust DEGs were then validated in GSE15605, and DEGs that were also statistically significant (q value < 0.01) in GSE15605 were used in following analyses. The identified DEGs were further validated in the Gene Expression Profiling Interactive Analysis (GEPIA) online database (http://gepia.cancer-pku.cn/)[21], which contains a large number of normal samples that were derived from the Genotype-Tissue Expression (GTEx) projects in addition to TCGA melanoma samples.

2.3. Pathway and functional enrichment analyses of DEGs

To gain more insights into the functions and biological processes of the DEGs, we utilized the R package *clusterProfiler* for Kyoto Encyclopedia of Genes and Genomes (KEGG) and gene ontology (GO) enrichment analyses[22]. Significant pathways and GO items were selected with FDR $q < 0.05$.

2.4. Identification and validation of prognostic gene signatures

DEGs that could be used to predict the OS of patients with melanoma were selected using the univariate Cox proportional hazards models in TCGA data set. Genes with $P < 0.05$ were then fitted in the multivariate LASSO Cox regression model with the R package *glmnet*[23]. The optimal λ value was determined by ten-fold cross validation that gives a minimum cross-validated error. Coefficients of genes without significant effect on OS were shrunk to zero. The correlations among significant genes were assessed using Spearman's correlation method. Then, the prognostic immune score (PIS) for each patient was constructed, which is the linear combination of the expression of genes and the corresponding coefficients estimated in LASSO model. The patients in TCGA data set were divided into high-risk group and low-risk group based on the median of PIS. The time of OS and disease-free survival (DFS) between the two groups were compared using Kaplan–Meier analyses and log-rank tests, separately. The identified prognostic gene signature was validated in an independent cohort GSE65904. PIS was calculated according to the expression of each identified gene and its associated coefficient obtained from the TCGA data set. Subsequently, the high-risk group and low-risk group were formed according to the median of PIS, and the time of OS and distant metastasis-free survival (DMFS) between the two groups were compared by Kaplan–Meier analyses and log-rank tests, separately. Since TCGA data set has relatively more complete clinical information than other data sets, we investigated whether prognostic value of PIS was independent of clinical baseline information using multivariate Cox proportional hazards models in TCGA data set. $P < 0.05$ was set as a cutoff for significant difference. All data were statistically analyzed with R software (version 3.4.4).

2.5. Exploring the associations between identified prognostic genes and tumor-associated leukocyte (TAL) subsets

Leukocyte compositions were inferred from the bulk tumor transcriptomes using CIBERSORT, which could estimate relative proportions of TAL from expression profiles of bulk tumors and outperform other TAL decomposition methods[24]. After applying CIBERSORT to TCGA data set, 22 distinct TAL subsets were obtained, and the correlation between each identified prognostic gene and the specific TAL was calculated using Spearman's rank correlation. Genes that had the largest absolute correlation coefficients with certain TAL subset among all TAL subsets were considered to have strong association with that TAL subset. In addition, melanoma subset was defined as the average expression of known melanoma markers (MLANA, S100A1, PAN2, SOX10, TYR, S100B, and MITF), and the association between each identified prognostic gene and melanoma subset was explored using Spearman's rank correlation.

2.6. Cell culture, stimulation, and cell transfection

A375 and B16F10 cells were purchased from ATCC. They were cultured in DMEM (01-052-1A, Biological Industries, Israel) cell culture medium with 10% fetal bovine serum (04-001-1ACS, Biological Industries, Israel). In cell culture experiments, transfection of LCP2 shRNA (GenePharma Biotechnology Company, Shanghai, China) was conducted based on the operation manual. Non-targeting shRNA was used as a control. shRNAs were transfected into A375 and B16F10 cells with Lipofectaminected i (L3000015, Invitrogen) according to corresponding instructions. For obtaining stable LCP2 knockdown cells, pMD2.G, psPAX2, and shRNA were cotransfected into HEK-293T cells with TurboFect (R0532, Thermo Fisher Scientific) based on the corresponding operation manual. RT-PCR was used for efficiency verification of transfection.

2.7. Animal studies

Female BALB/c nude mice (4-6 weeks old) and female C57BL/6 mice (6-8 weeks old) were used for A375 experiments and B16F10 experiments, respectively. 1ect^6 A375 or B16F10 cells (0.1 mL) were subcutaneously implanted to female nude or C57BL/6 mice. To determine tumor growth, a caliper was used to record the tumor sizes every 5 days. All animal studies were evaluated and approved by the Institutional Animal Care and Use Committee of Xiangya Hospital, Central South University (No. 2022020685).

2.8. RT-qPCR

Tripure (Bio Teke, RP1002) and a reverse transcription kit (HiScript Q RT, Vazyme, R223-01) were used to extract the total RNA and reverse-transcribe RNA into cDNA, respectively. The PCR system was prepared according to the SYBR qPCR Mix kit (Bimake, B21703). The relatively expression levels of LCP2 and IRF5 were detected by normalization to GAPDH using ΔΔCt method. The primer sequences used for the RT-qPCR are listed in Table 1.

2.9. Flow cytometry

2% paraformaldehyde solution in phosphate-buffered saline (PBS) was used for cell fixation, then stained with fluorescent-labeled antibodies for cell-surface markers for 1 h at 4°C in the dark, and subsequently washed and resuspended for flow cytometry analysis. The antibodies used in this part are as follows: anti-mouse CD4 FITC (100406), anti-mouse CD45 APC (103112), anti-mouse CD4 PE (100407), anti-mouse/human Granzyme B PE (372208), AF647 anti-human/mouse Granzyme B antibody (515405), and anti-mouse CD8 APC (100766). The FACSCalibur (BD Biosciences) and FlowJo software (Version 10.4) were used for flow cytometry analysis and data analysis, respectively.

Table 1. Primer sequences used for the RT-qPCR

Gene	Primer sequence (5' to 3')
LCP2	
Forward	AGAATGTCCCGTTTCGCTCAG
Reverse	TGCTCCTTCTCTCTTCGTTCTT
IRF5	
Forward	AGAGACAGGGAAGTACACTGAAG
Reverse	TGGAAGTCACGGCTTTTGTTAAG
GAPDH	
Forward	CTCTGCTCCTCCTGTTCGAC
Reverse	GCCCAATACGACCAAATCC

RT-qPCR: Real time-quantitative polymerase chain reaction

2.10. Identification of differentially expressed genes associated with LCP2

To further explore the mechanism of LCP2 regulating progression of melanoma, we analyzed the DEGs between LCP2 knockdown group and control group. Ribo-Zero rRNA removal kit was used to remove rRNA from 1 μg of total RNA. TruSeq RNA sample prep kit (Illumina) was used to generate sequencing libraries, and then sequenced as 151-bp paired-end reads using an Illumina HiSeq X Ten platform, with $P < 0.05$ and $|\text{foldchange}| > 1$ as cutoff value.

2.11. Statistical analysis

All data from the experiments are expressed as mean ± SEM. Statistical analyses of these data were performed using GraphPad Prism 9 (GraphPad Software, La Jolla, CA) with an unpaired Student's *t*-test or Tukey's multiple comparison. $P < 0.05$ was set as a cutoff for significant difference.

3. Results

3.1. Identification of DEGs

Among the 2070 immune-centric genes, there were 1582 immune-centric genes in GSE3189 data set and 1842 in GSE31879 data set. Based on the criteria of FDR q value < 0.01, the number of DEGs between melanoma and nevus, melanoma and normal skin, and melanoma and melanocyte were 720, 801, and 335, respectively, in GSE3189 and GSE31879 data sets. The intersection of these three comparisons was 105, which were differently expressed in all three comparisons (Figure 1A). Among 105 genes, 47 were confirmed as DEGs in GSE15605 (Figure 1B). GO functional enrichment analysis showed that the changes in 47 genes were mainly related to the biological processes of neutrophil and autophagy (Figure 1C). KEGG pathway enrichment analysis demonstrated that these 47 DEGs were significantly involved in lysosome, B-cell receptor

signaling pathways, T-cell receptor signaling pathway, Fc epsilon RI signaling pathway, and so on (Figure 1D).

3.2. Identification of prognostic gene signature

Twelve out of 47 DEGs were statistically significant in predicting the OS in univariate Cox proportional hazards models in TCGA data set (Figure 2). Among them, *BLNK*, *DAPP1* and *IL18* were downregulated, and other genes were upregulated in melanoma samples compared to normal samples. These genes were then fitted in the LASSO model, and ten of them that were predictive of OS were selected (Figure 3A). These genes include *BLNK*, *CD81*, *CLEC4E*, *CPPED1*, *IL18*, *ISG20*, *LCP2*, *MGRN1*, *RAB5C,* and *TRIM32*. Our results revealed that elevated expression of CD81, IL18, MGRN1, RAB5C, and TRIM32 were associated with worse OS for melanoma, and elevated expression of BLNK, CLEC4E, CPPED1, ISG20, and LCP2 were associated with better prognosis for melanoma. In addition, there were strong correlations among BLNK, IL18, CLEC4E, and LCP2 (Figure 3B). To investigate whether the prognostic value of the identified ten-gene signature was independent of clinical characteristics, we employed univariate and multivariate Cox regression models to consider the covariates of age, sex, sample type, tumor stage, Breslow thickness, and ulceration in TCGA data set. Since sex was not statistically significant in univariate Cox regression models for predicting both OS and DFS, it was excluded when fitting multivariate Cox regression models. Results showed that PIS was statistically significant for predicting OS and DFS after adjusting for effects of several clinical information (Figure 3C and D & Tables S2 and S3).

3.3. Construction and validation of PIS

The PIS was calculated based on the linear combination of selected ten genes and corresponding coefficients, and patients with melanoma in TCGA data set were divided into high-risk group (N = 235) and low-risk group (N = 236). The OS of high-risk group was significantly worse than that of low-risk group (log-rank P = 3e-10, HR: 2.343, 95% CI:

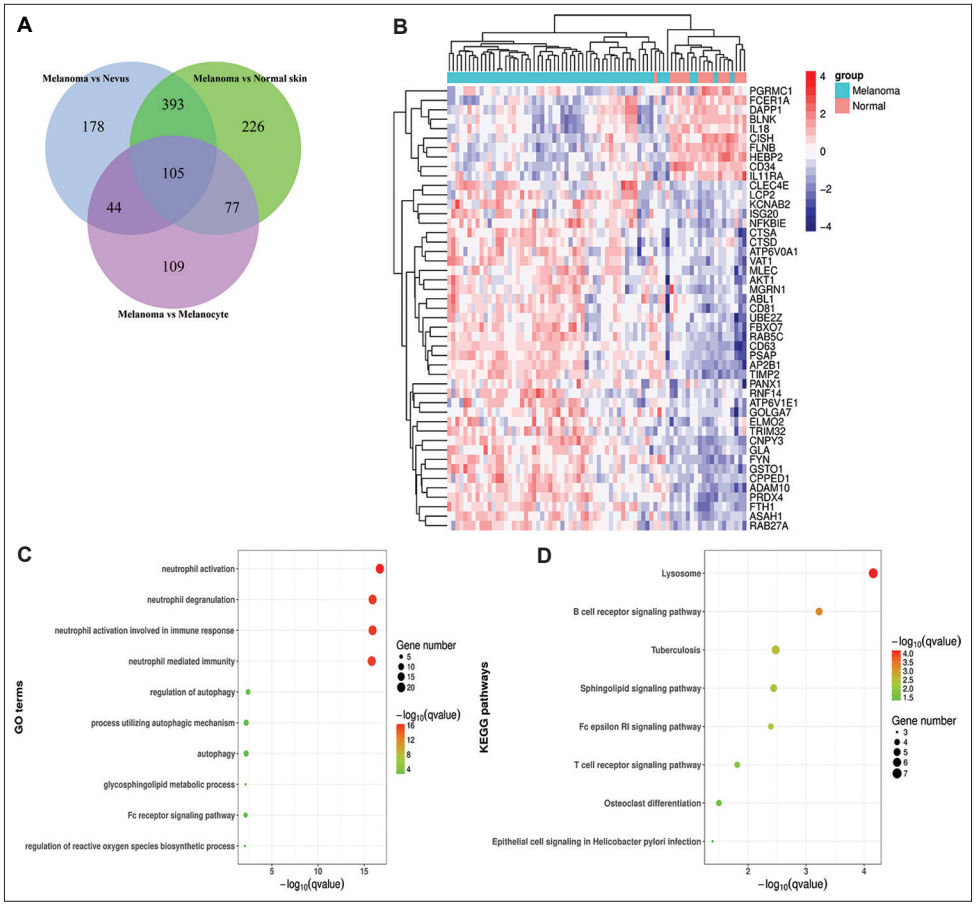


Figure 1. Identification of DEGs. (A) Overlapping DEGs shared between melanoma and benign skin nevus, melanoma and normal skin tissue, and melanoma and normal melanocyte. (B) Heatmap of DEGs. (C) GO functional enrichment analysis (top 10 results). (D) KEGG pathway enrichment analysis (top 10 results).
DEGs: Differentially expressed genes; KEGG: Kyoto Encyclopedia of Genes and Genomes; GO: Gene ontology.

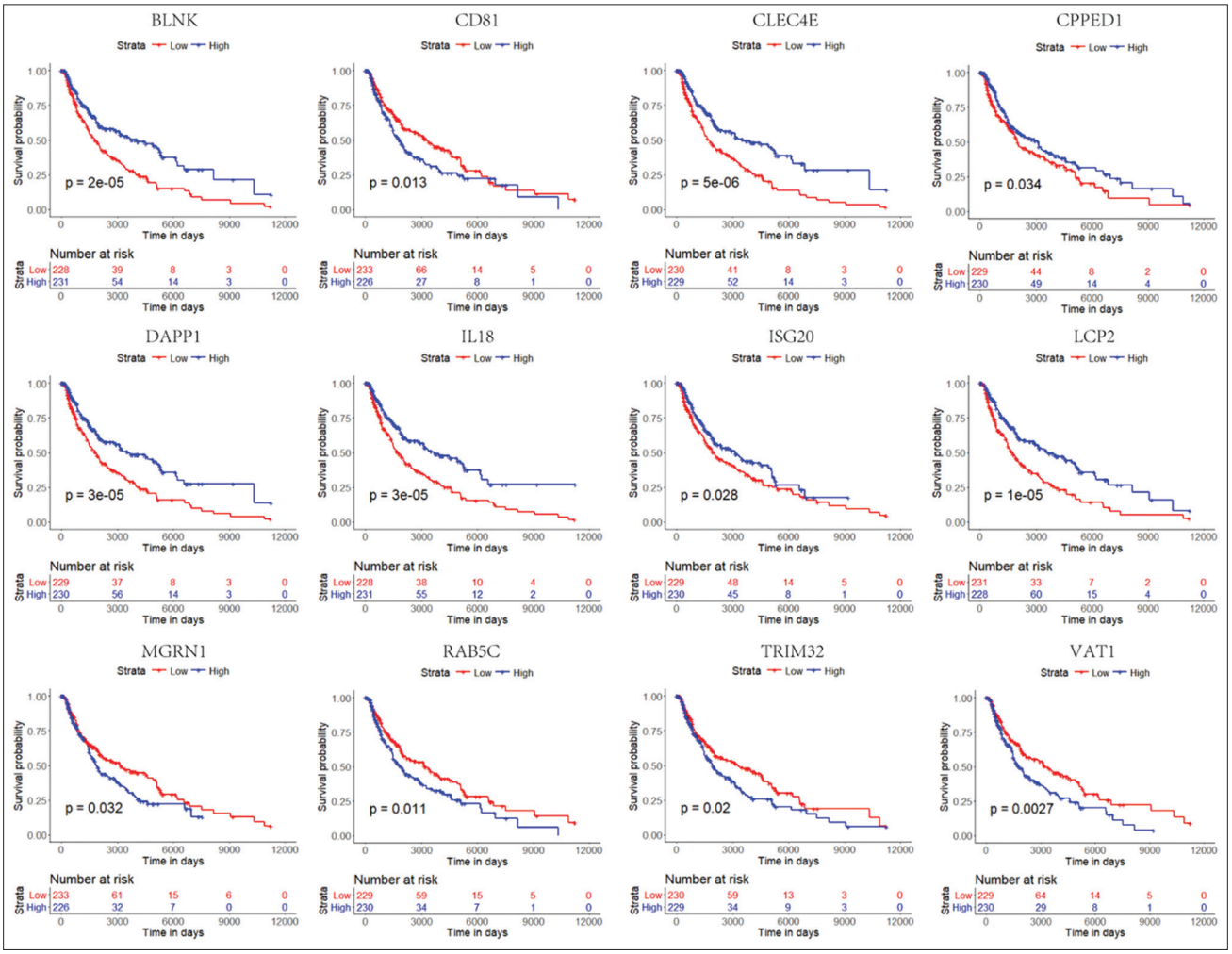


Figure 2. Univariate survival analysis for DEGs in TCGA data set.
DEGs: Differentially expressed genes; TCGA: The Cancer Genome Atlas.

1.785 – 3.076, Figure 4A), with the median survival time of 1628 and 4601 days, respectively. Meanwhile, our results showed that the DFS of high-risk group was significantly worse than that of low-risk group (log-rank P = 8e-07, HR: 2.895, 95% CI: 1.867 – 4.489, Figure 4B), with the median survival time of 2195 and 6299 days, respectively. To explore the robustness of ten-gene signature for predicting the survival of melanoma, we externally validated the prognostic ability of ten-gene signature in an independent GSE65904 data set. Results showed that the OS of high-risk patients in GSE65904 was significantly worse than that of low-risk patients (log-rank P = 0.0036, HR: 1.786, 95% CI: 1.202 – 2.653 days, Figure 4C), with the median survival time of 629 and 1404, respectively. In addition, patients in high-risk group had significantly worse DMFS than those in low-risk group (log-rank P = 0.0082, HR: 1.786, 95% CI: 1.155 – 2.762, Figure 4D), with the median survival time of 379 and 1401 days, respectively.

3.4. Associations between identified prognostic genes and TAL subsets

The associations between the selected ten prognostic genes and the specific TAL were calculated using Spearman's rank correlation. Genes that had the largest absolute correlation coefficients with certain TAL subset among all TAL subsets were considered to have strong association with that TAL subset. Results showed that LCP2, ISG20, and CLEC4E expression were significantly positively correlated with $CD8^+$ T-cells. CD81 and MGRN1 expression were significantly positively correlated with Treg cells, while BLNK and IL-18 expression were significantly negatively correlated with M0 macrophages. In addition, RAB5C and TRIM32 expression had strong association with B-cells and natural killer cells, respectively (Figure 5). Given the important role of LCP2 in the immune system, we focused our efforts on investigating LCP2 in the subsequent studies.

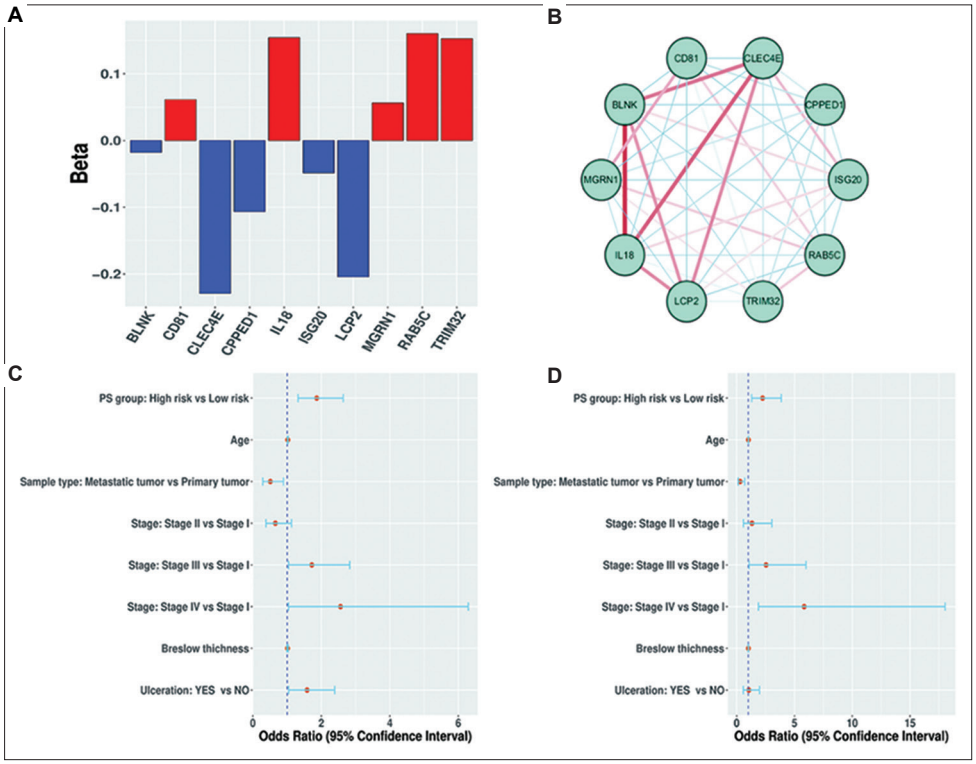


Figure 3. Identification of prognostic gene signature. (A) The identified prognostic gene signature in LASSO model. (B) Correlations among identified prognostic genes. (C) Multivariate analysis for the association between PIS and OS after adjusting for covariates. (D) Multivariate analysis for the association between PIS and DFS after adjusting for covariates.
PIS: Prognostic immune score; OS: Overall survival.

3.5. LCP2 inhibited the growth of melanoma possibly through the positive regulation of IRF5 signaling pathway to activate CD8⁺ T-cells

To determine the function of LCP2 in melanoma, we established the LCP2 knockdown mouse tumor model. At first, we validated the knockdown efficacy of LCP2 in B16F10 cell through RT-qPCR (Figure 6A). It was obvious to see that knockdown of LCP2 significantly promoted the tumor growth (Figure 6B–D) in wild-type mice but had no effect on tumor sizes in nude mice, indicating the negative correlation between LCP2 and melanoma growth, as well as the importance of LCP2 in the tumor immune microenvironment (Figure 6E). Furthermore, flow cytometry analysis of shLCP2 melanoma cells showed no significantly changes of $CD4^+$ and $CD8^+$ T-cells, but remarkable reduction of Granzyme B-positive cells, which implied that LCP2 loss decreased the activity of $CD8^+$ T-cells and led to the promotion of tumor growth (Figure 6F–J). Moreover, to further explore the underlying mechanism of LCP2 regulating the activity of $CD8^+$ T-cells, DEGs between shLCP2 group and control group were analyzed. In total, 846 DEGs were found with $P < 0.05$ and $|\text{foldchange}| > 1$, among which 407 DEGs were upregulated and 439 DEGs were downregulated. The volcano plot of DEGs showed that the IRF5 was significantly downregulated in the shLCP2 group (Figure 6K). All the DEGs in this part are listed in **Table S4**. Similar result was also noted in RT-qPCR experiment (Figure 6L), suggesting that LCP2 may positively regulate the IRF5 signaling pathway to activate $CD8^+$ T-cells and then inhibit the growth of melanoma (Figure 6M).

4. Discussion

Melanoma is known to be the most lethal type of skin cancer. The advent of immunotherapy has revolutionized the status of clinical therapies of melanoma, which brought new hope to these patients. However, only a small proportion of patients are responders. Therefore, novel prognostic and immune-related biomarkers are urgently needed to guide the development of melanoma treatments. In the present study, RNA-seq data of cutaneous melanoma from the public database were used for identifying prognostic gene signatures. KEGG pathway enrichment analysis showed that 47 DEGs were significantly involved in lysosome, B-cell receptor signaling pathways, T-cell receptor signaling pathway, and Fc epsilon RI signaling pathway, indicating that these signaling pathways play an important role in melanoma.

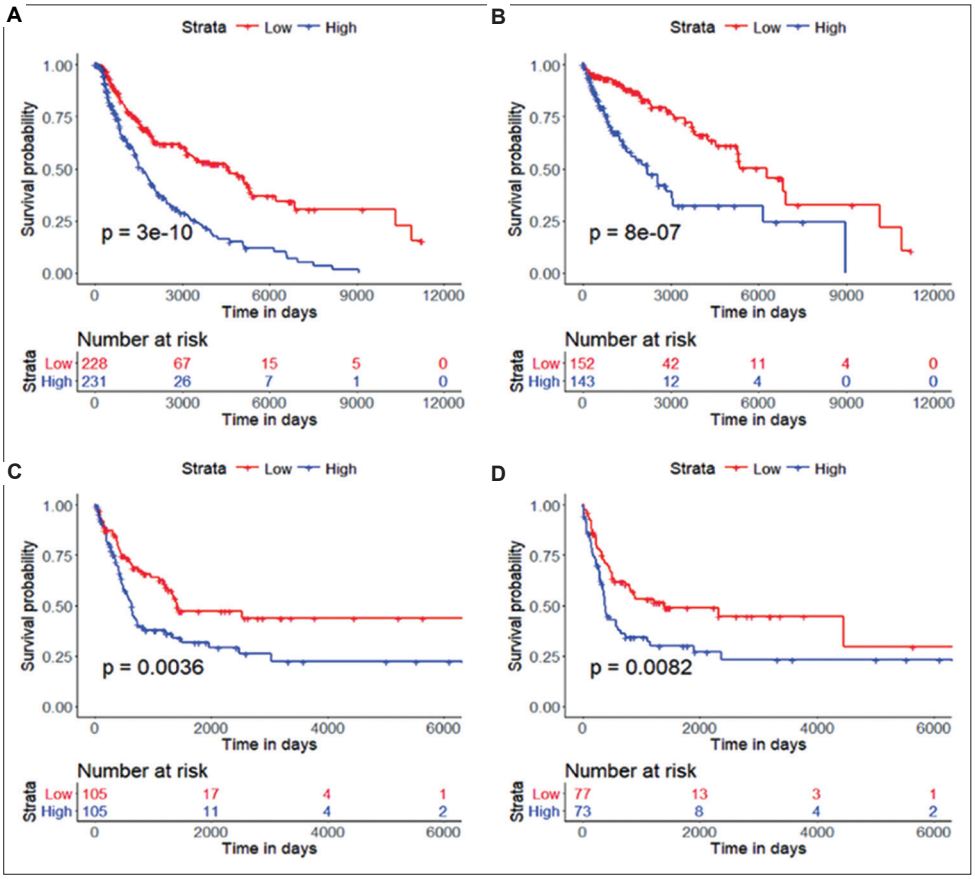


Figure 4. Survival curves for high- and low-risk patients based on PIS. (A) Survival curves for DMFS in GSE65904 data set. (B) Survival curves for OS in GSE65904 data set. (C) Survival curves for DFS in TCGA data set. (D) Survival curves for OS in TCGA data set.
PIS: Prognostic immune score; OS: Overall survival; DMFS: Distant metastasis-free survival; DFS: Disease-free survival; TCGA: The Cancer Genome Atlas.

Furthermore, ten (*BLNK*, *CD81*, *CLEC4E*, *CPPED1*, *IL18*, *ISG20*, *LCP2*, *MGRN1*, *RAB5C*, and *TRIM32*) out of the 47 DEGs were statistically significant in predicting the OS in univariate Cox proportional hazards models and LASSO model in TCGA data set. Our results revealed that elevated expression of CD81, IL18, MGRN1, RAB5C, and TRIM32 were associated with worse OS in melanoma patients, and elevated expression of BLNK, CLEC4E, CPPED1, ISG20, and LCP2 were associated with better prognosis in melanoma patients. The PIS was calculated based on the linear combination of the expression of selected ten genes, and the PIS was statistically significant in predicting OS and DFS in melanoma patients after adjusting for several clinical covariates.

At present, numerous studies have reported the important roles of various tumor-infiltrating immune cells in melanoma[25-28]. To investigate the association between the selected ten prognostic genes and tumor-infiltrating immune cells, we applied CIBERSORT to TCGA data set and obtained 22 distinct TAL subsets, and used Spearman's rank correlation to analyze the correlation between each identified prognostic gene and the specific TAL. We found that these identified prognostic genes were mainly correlated with $CD8^+$ T cells, Treg cells, B cells, M0 macrophages, and natural killer cells. It is worth noting that the expression level of LCP2 was positively associated with $CD8^+$ T-cells.

A few studies have shown that LCP2 was differentially expressed in many different types of tumors and was correlated with prognosis in numerous cancers[10-12]. Moreover, LCP2 was reported essential for normal T-cell development and activation[14]. In our present study, the bioinformatics analyses revealed that high LCP2 expression in melanoma patients was statistically significant for predicting the OS in univariate Cox proportional hazards models in TCGA data set and was associated with better prognosis in melanoma patients. In addition, we found that LCP2 expression was significantly positively correlated with $CD8^+$ T-cells, indicating that LCP2 could be a potential immunotherapy target. Moreover, given the important role of LCP2 in the immune system as reported in numerous published studies, we hence focused our efforts on investigating LCP2 in the subsequent studies. The *in vivo*

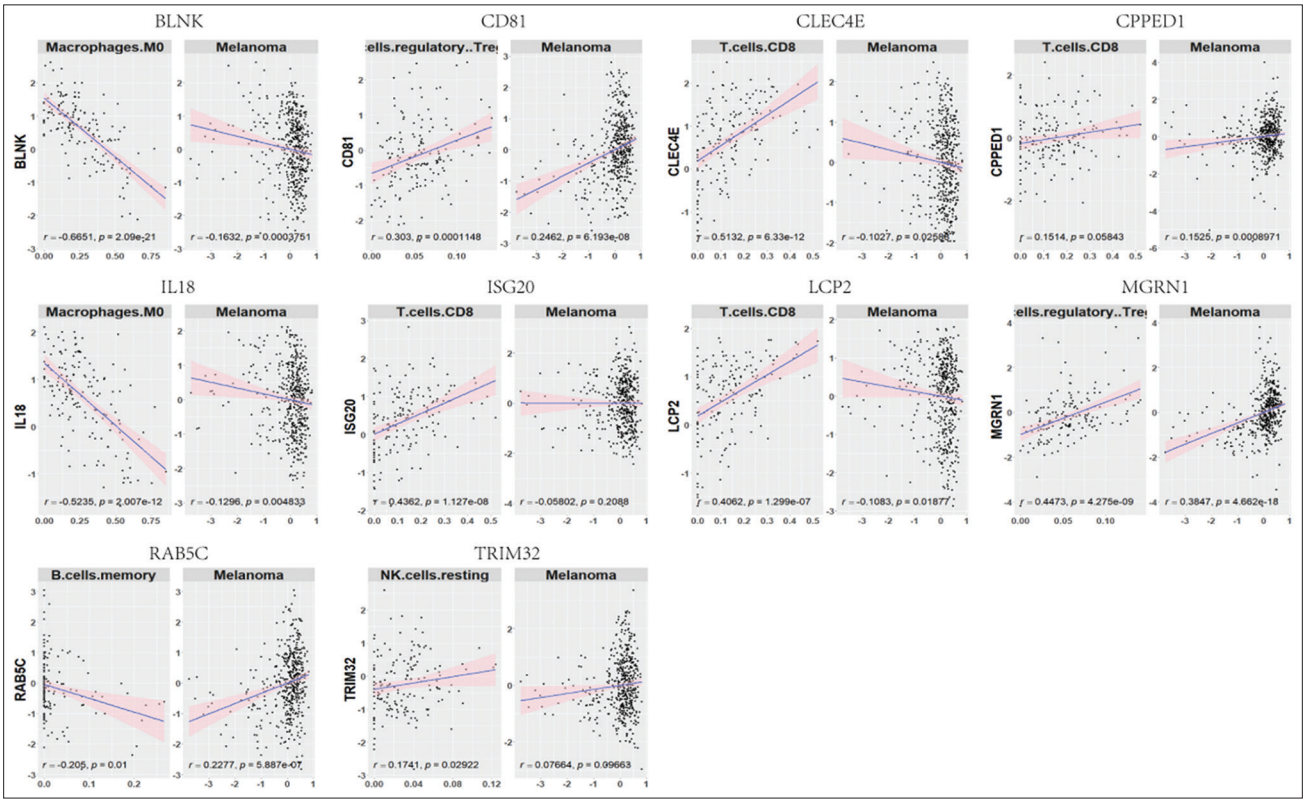


Figure 5. Association between identified prognostic genes and TAL subsets and melanoma.
TAL: Tumor-associated leukocyte.

experiment showed that knockdown of LCP2 significantly promoted the progression of melanoma in wild-type mice but had no effect on tumor sizes in nude mice, indicating the negative correlation between LCP2 and melanoma growth, as well as the importance of LCP2 in the tumor immune microenvironment. The result of flow cytometry analysis directly confirmed the positive correlation between LCP2 expression and $CD8^+$ T-cell activity. However, the pathway by which LCP2 regulates T-cell activity is unknown.

To explore the mechanism through which LCP2 regulates T-cell activity, DEGs of shLCP2 group versus control group were analyzed in this study, and we found that IRF5 expression was significantly downregulated. Interferon regulatory factors (IRFs) are transcriptional mediators of type 1 interferon signaling pathway induced by pathogens and viruses, which are also involved in immune response, apoptosis, cell growth regulation, and oncogenesis[29-31]. Some members of the IRFs have been shown to be involved in regulating development and function of the immune cells[32-34]. IRF5, as a member of IRFs, has been reported to play a key role in immune regulation of autoimmune diseases and inflammatory responses, which therefore attracted much attention in recent years. In addition, it has been revealed that IRF5 is involved in the activation of inflammatory cytokines and chemokines that are important for recruitment of T-cells[35,36]. Moreover, the intratumoral IRF5 deletion in breast cancer cells dysregulated secretion of many chemokines and cytokines, leading to the inaccurate and untimely transport of immune cells to the tumor sites[37]. Takaoka *et al.* found that Irf5 knockout mice were unable to secrete proinflammatory cytokines (such as tumor necrosis factor α [TNF-α], IL-6, and IL-12), and exhibited resistance toward endotoxic shock induced by lipopolysaccharide, indicating that IRF5 was generally involved in the downstream of TLR-MyD88 signaling pathway and induced the gene expression of proinflammatory cytokines[38]. Moreover, studies have shown that most of the chemokines induced by virus in cells showed lymphocyte chemotactic activity in the case of overexpression IRF5[35], which therefore were significant for T-lymphocyte recruitment, indicating a possible key role of IRF5 in lymphocyte trafficking. Therefore, we speculated the key bridge linking of IRF5 between LCP2 and $CD8^+$T-cell. In our study, the expression of IRF5 was remarkably decreased in LCP2 knockdown B16F10 cells. Taking together, we speculated that high expression of LCP2 in melanoma upregulated the IRF5 expression and IRF5 then mediated the secretion of proinflammatory

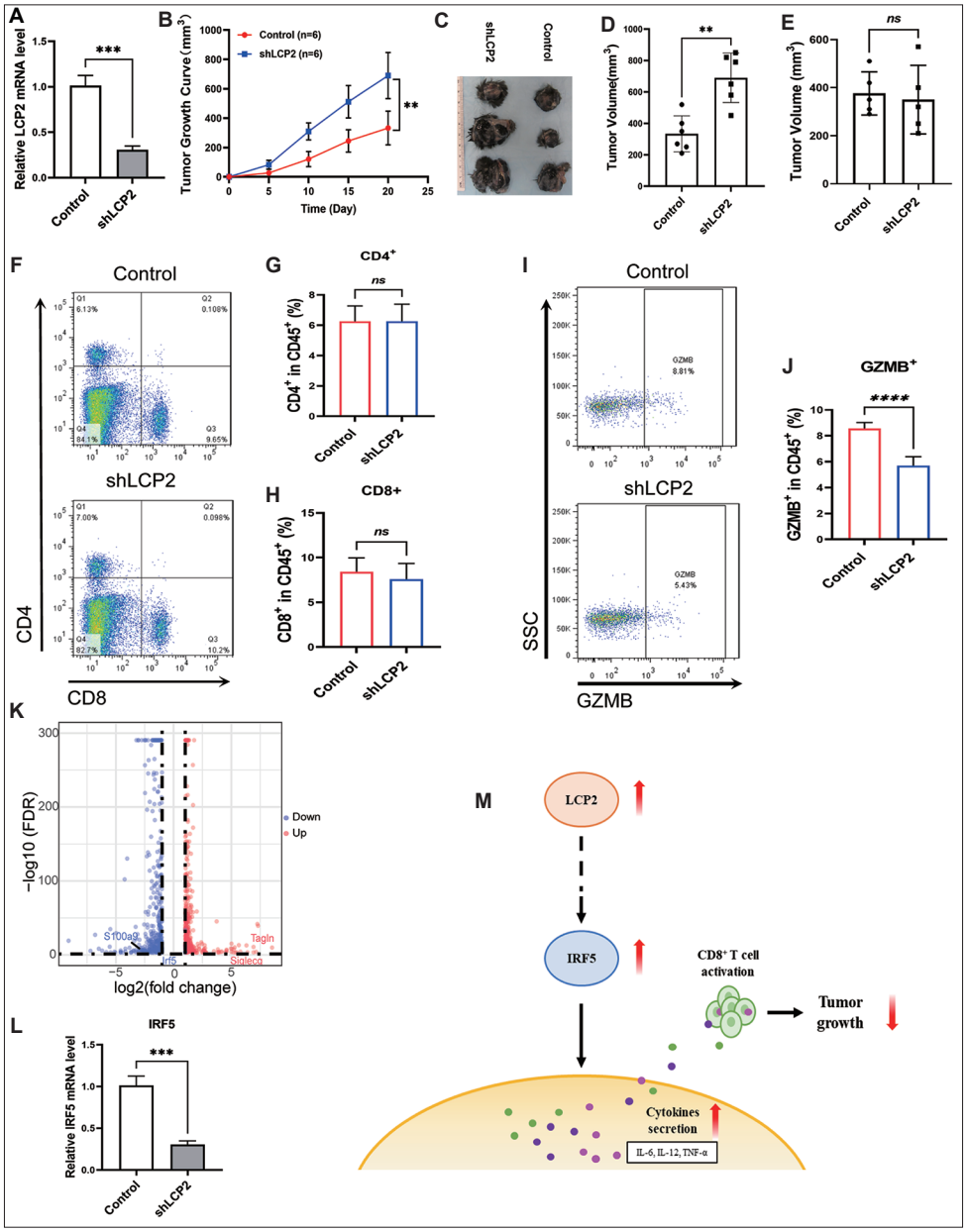


Figure 6. Analysis of underlying mechanism of LCP2 knockdown suppressing the growth of melanoma. (A) RT-qPCR analyses of LCP2 in control and LCP2 knockdown (shLCP2) B16F10 cells (n = 3). (B) B16F10 cells and shLCP2 B16F10 cells (10^6) were injected subcutaneously into C57BL/6 mice. Tumor volume was measured every 5 days and calculated using this formula: (length×width²)/2. (C) Representative tumors were resected and photographed at day 20. Tumor volume in C57BL/6 mice (D) and in BALB/c nude mice € were recorded at day 20 (n = 6 in C57BL/6 mice group, n = 5 in BALB/c nude mice group). Flow cytometry analyses (F) and quantitative analyses of CD4⁺ (G) and CD8⁺ cells (H), and flow cytometry (I) and quantitative analysis of Granzyme B-positive (GZMB⁺) cells (J) in the melanoma tumor from immunocompetent wild-type BALB/c mice with subcutaneous injection of shLCP2 and control B16F10 cells. (K) Volcano plot of DEGs shared between control group and shLCP2 group (significantly upregulated genes are denoted by red nodes; significantly downregulated genes are denoted by blue nodes). (L) RT-qPCR analyses of IRF5 in control and shLCP2 B16F10 cells (n = 3). (M) A schematic diagram showing the hypothetical mechanism of high LCP2 expression positively regulating IRF5 signaling pathway to activate tumor-infiltrating CD8⁺ T cells and then inhibit the growth of melanoma. Tukey's multiple comparison or Student's t-test was used to calculate p values for results shown in this figure.

ns: Not significan; *P < 0.05; **P < 0.01; ***P < 0.001; ****P < 0.0001; LCP2: Lymphocyte cytosolic protein 2; RT-qPCR: Real time-quantitative polymerase chain reaction; DEGs: Differentially expressed genes; IRF5: Interferon regulatory factor 5.

cytokines and chemokines to activate $CD8^+$ T lymphocytes, which finally suppressed the growth of melanoma.

5. Conclusions

LCP2 is a novel prognostic biomarker of melanoma, which could positively regulate the IRF5 signaling pathway to activate tumor-infiltrating $CD8^+$ T-cells and then inhibit the growth of melanoma. Nevertheless, it is important to point out that there are some limitations in our study. First, the potential association between LCP2 and IRF5 is unclear, which needs to be systematically and deeply explored *in vitro* and *in vivo*. Second, more public data on melanoma patients who received immunotherapy should be included for bioinformatics analysis in this study to investigate prognostic significance of LCP2 in these patients.

Acknowledgments

None.

Funding

This study was supported by grants from General Program, the National Natural Science Foundation of China (No. 81874138, 82073020 and 81903222).

Conflict of interest

The authors declare no conflicts of interest.

Author contributions

Conceptualization: Mingzhu Yin
Data curation: Hongyin Sun, Kui Deng
Investigation: Hongyin Sun, Kui Deng
Validation: Xingchen Zhou, Dongsheng Cao, Yan Cheng
Writing – original draft: Hongyin Sun, Kui Deng, Mingzhu Yin
Writing – review & editing: Xiang Chen, Mingzhu Yin

Ethics approval and consent to participate

All the procedures of animal study were evaluated and approved by the Institutional Animal Care and Use Committee of Xiangya Hospital, Central South University (No. 2022020685).

Consent for publication

Not applicable.

Availability of data

The data used to support the findings of this study are available from the corresponding author on reasonable request.

References

1. Torre LA, Bray F, Siegel RL, *et al.*, 2015, Global cancer statistics, 2012. *CA Cancer J Clin*, 65(2): 87–108.
https://doi.org/10.3322/caac.21262
2. Schadendorf D, Fisher DE, Garbe C, *et al.*, 2015, Melanoma. *Nat Rev Dis Primers*, 1: 15003.
https://doi.org/10.1038/nrdp.2015.3
3. Luke JJ, Flaherty KT, Ribas A, *et al.*, 2017, Targeted agents and immunotherapies: Optimizing outcomes in melanoma. *Nat Rev Clin Oncol*, 14(8): 463.
https://doi.org/10.1038/nrclinonc.2017.43
4. Redman JM, Gibney GT, Atkins MB, 2016, Advances in immunotherapy for melanoma. *BMC Med*, 14(1): 20.
https://doi.org/10.1186/s12916-016-0571-0
5. D'Arcangelo D, Giampietri C, Muscio M, *et al.*, 2018, WIPI1, BAG1, and PEX3 autophagy-related genes are relevant melanoma markers. *Oxidat Med Cell Longev*, 2018: 1471682.
https://doi.org/10.1155/2018/1471682
6. Gerami P, Cook RW, Wilkinson J, *et al.*, 2015, Development of a prognostic genetic signature to predict the metastatic risk associated with cutaneous melanoma. *Clin Cancer Res*, 21(1): 175–183.
https://doi.org/10.1158/1078-0432.CCR-13-3316
7. Zhao Y, Schaafsma E, Gorlov IP, *et al.*, 2018, A leukocyte infiltration score defined by a gene signature predicts melanoma patient prognosis. *Mol Cancer Res*, 17(1): 109filtra.
https://doi.org/10.1158/1541-7786.MCR-18-0173
8. Clements JL, Ross-Barta SE, Tygrett LT, *et al.*, 1998, SLP-76 expression is restricted to hemopoietic cells of monocyte, granulocyte, and T lymphocyte lineage and is regulated during T cell maturation and activation. *J Immunol*, 161: 3880–3889.
9. Jumaa H, Wollscheid B, Mitterer M, *et al.*, 1999, Abnormal development and function of B lymphocytes in mice deficient for the signalling adaptor protein SLP-65. *Immunity*, 11: 547–554.
https://doi.org/10.1016/s1074-7613(00)80130-2
10. Zhang J, Wang L, Xu X, *et al.*, 2020, Transcriptome-based network analysis unveils eight immune-related genes as molecular signatures in the immunomodulatory subtype of triple negative breast cancer. *Front Oncol*, 10: 1787.
https://doi.org/10.3389/fonc.2020.01787
11. Huo Y, Zhang K, Han S, *et al.*, 2021, Lymphocyte cytosolic protein 2 is a novel prognostic marker in lung adenocarcinoma. *J Int Med Res*, 49(11): 3000605211059681.
https://doi.org/10.1177/03000605211059681
12. Wang Z, Peng M, 2021, A novel prognostic biomarker LCP2

correlates with metastatic melanoma-infiltrating CD8 T cells. *Sci Rep*, 11(1): 9164.

https://doi.org/10.1038/s41598-021-88676-9

13. Koretzky GA, Abtahian F, Silverman MA, 2006, SLP76 and SLP65: Complex regulation of signalling in lymphocytes and beyond. *Nat Rev Immunol*, 6(1): 67–78.

https://doi.org/10.1038/nri1750

14. Navas VH, Cuche C, Alcover A, *et al*., 2017, Serine phosphorylation of SLP76 is dispensable for T cell development but modulates helper T cell function. *PLoS One*, 12(1): e0170396.

https://doi.org/10.1371/journal.pone.0170396

15. Sommers CL, Menon RK, Grinberg A, *et al*., 2001, Knock-in mutation of the distal four tyrosines of linker for activation of T cells blocks murine T cell development. *J Exp Med*, 194(2): 135–142.

https://doi.org/10.1084/jem.194.2.135

16. Maltzman JS, Kovoor L, Clements JL, *et al*., 2005, Conditional deletion reveals a cell-autonomous requirement of SLP-76 for thymocyte selection. *J Exp Med*, 202(7): 893–900.

https://doi.org/10.1084/jem.20051128

17. Siggs OM, Miosge LA, Daley SR, *et al*., 2015, Quantitative reduction of the TCR adapter protein SLP-76 unbalances immunity and immune regulation. *J Immunol*, 194(6): 2587–2595.

https://doi.org/10.4049/jimmunol.1400326

18. Fabregat A, Jupe S, Matthews L, *et al*., 2017, The reactome pathway knowledgebase. *Nucleic Acids Res*, 46(D1): D649–D655.

https://doi.org/10.1093/nar/gkx1132

19. Hastie T, Tibshirani R, Narasimhan B, *et al*., 2016, Impute: Imputation for microarray data. *Oral History Rev*, 2016.

20. Benjamini Y, Hochberg Y, 1995, Controlling the false discovery rate: A practical and powerful approach to multiple testing. *J R Stat Soc Ser B Methodol*, 57(1): 289–300.

https://doi.org/10.1111/j.2517-6161.1995.tb02031.x

21. Tang Z, Li C, Kang B, *et al*., 2017, GEPIA: A web server for cancer and normal gene expression profiling and interactive analyses. *Nucleic Acids Res*, 45(W1): W98–W102.

https://doi.org/10.1093/nar/gkx247

22. Yu G, Wang LG, Han Y, *et al*., 2012, clusterProfiler: An R package for comparing biological themes among gene clusters. *OMICS*, 16(5): 284–287.

https://doi.org/10.1089/omi.2011.0118

23. Friedman J, Hastie T, Tibshirani R, 2009, Glmnet: Lasso and Elastic-net Regularized Generalized Linear Models. R Package Version, 1(4).

24. Newman AM, Liu CL, Green MR, *et al*., 2015, Robust enumeration of cell subsets from tissue expression profiles. *Nat Methods*, 12(5): 453–457.

https://doi.org/10.1038/nmeth.3337

25. Balatoni T, Mohos A, Papp E, *et al*., 2018, Tumor-infiltrating immune cells as potential biomarkers predicting response to treatment and survival in patients with metastatic melanoma receiving ipilimumab therapy. *Cancer Immunol Immunother*, 67(1): 141–151.

https://doi.org/10.1007/s00262-017-2072-1

26. Liu D, 2019, CAR-T "the living drugs", immune checkpoint inhibitors, and precision medicine: A new era of cancer therapy. *J Hematol Oncol*, 12(1): 113.

https://doi.org/10.1186/s13045-019-0819-1

27. Dabrosin N, Juul KS, Georgsen JB, *et al*., 2019, Innate immune cell infiltration in melanoma metastases affects survival and is associated with BRAFV600E mutation status. *Melanoma Res*, 29(1): 30–37.

https://doi.org/10.1097/CMR.0000000000000515

28. Fu X, Yin M, 2022, Monocytes in tumor: The perspectives of single-cell analysis. *Tumor Discov*, 1(1): 4.

https://doi.org/10.36922/td.v1i1.4

29. Honda K, Taniguchi T, 2006, IRFs: Master regulators of signalling by Toll-like receptors and cytosolic pattern-recognition receptors. *Nat Rev Immunol*, 6(9): 644–658.

https://doi.org/10.1038/nri1900

30. Honda K, Takaoka A, Taniguchi T, 2006, Type I interferon [corrected] gene induction by the interferon regulatory factor family of transcription factors. *Immunity*, 25(3): 349–360.

https://doi.org/10.1016/j.immuni.2006.08.009

31. Tamura T, Yanai H, Savitsky D, *et al*., 2008, The IRF family transcription factors in immunity and oncogenesis. *Annu Rev Immunol*, 26: 535–584.

https://doi.org/10.1146/annurev.immunol.26.021607.090400

32. Lohoff M, Mak TW, 2005, Roles of interferon-regulatory factors in T-helper-cell differentiation. *Nat Rev Immunol*, 5(2): 125–135.

https://doi.org/10.1038/nri1552

33. Battistini A, 2009, Interferon regulatory factors in hematopoietic cell differentiation and immune regulation. *J Interferon Cytokine Res*, 29(12): 765–780.

https://doi.org/10.1089/jir.2009.0030

34. Zhao GN, Jiang DS, Li H, 2015, Interferon regulatory factors: At the crossroads of immunity, metabolism, and disease. *Biochim Biophys Acta Mol Basis Dis*, 1852(2): 365–378.

https://doi.org/10.1016/j.bbadis.2014.04.030

35. Barnes BJ, Kellum MJ, Field AE, *et al*., 2002, Multiple

regulatory domains of IRF-5 control activation, cellular localization, and induction of chemokines that mediate recruitment of T lymphocytes. *Mol Cell Biol*, 22(16): 5721–5740.

https://doi.org/1128/MCB.22.16.5721-5740.2002

36. Kaur A, Lee LH, Chow SC, *et al*., 2018, IRF5-mediated immune responses and its implications in immunological disorders. *Int Rev Immunol*, 37(5): 229–248.

https://doi.org/10.1080/08830185.2018.146962

37. Pimenta EM, De S, Weiss R, *et al*., 2015, IRF5 is a novel regulator of CXCL13 expression in breast cancer that regulates CXCR5(+) B-and T-cell trafficking to tumor conditioned media. *Immunol Cell Biol*, 93(5): 486–499.

https://doi.org/10.1038/icb.2014.110

38. Takaoka A, Yanai H, Kondo S, *et al*., 2005, Integral role of IRF-5 in the gene induction programme activated by Toll-like receptors. *Nature*, 434(7030): 243–249.

https://doi.org/10.1038/nature03308